Journal of the Korean Electrochemical Society
Vol. 13, No. 1, 2010, 10-18

Review

Dye-Sensitized Metal Oxide Nanostructures and Their Photoelectrochemical Properties

Nam-Gyu Park*

School of Chemical Engineering, Sungkyunkwan University, Suwon 440-746, Korea

(Received February 2, 2010 : Accepted February 16, 2010)

Abstract : Nanostructured metal oxides have been widely used in the research fields of photoelectrochemistry, photochemistry and opto-electronics. Dye-sensitized solar cell is a typical example because it is based on nanostructured TiO_2. Since the discovery of dye-sensitized solar cell in 1991, it has been considered as a promising photovoltaic solar cell because of low-cost, colorful and semitransparent characteristics. Unlike p-n junction type solar cell, dye-sensitized solar cell is photoelectrochemical type and is usually composed of the dye-adsorbed nanocrystalline metal oxide, the iodide/tri-iodide redox electrolyte and the Pt and/or carbon counter electrode. Among the studied issues to improve efficiency of dye-sensitized solar cell, nanoengineering technologies of metal oxide particle and film have been reviewed in terms of improving optical property, electron transport and electron life time.

Keywords : Dye sensitized, Solar cell, Nano structure, Panchromatic

1. Introduction

According to the speech by Richard Smalley, the Nobel Prize winner in Chemistry in 1996, the most important issue will be the energy among the top ten most pressing problems that humanity must solve in next 50 years.[1] He cited predictions that the world would require 30-60 terawatts in the year 2050 and most of this energy will be supplied by renewable energies. He also expected that usages of fossil fuels such as petroleum will decline because of not only carbon dioxide emission accelerating global warming but also shortage. Therefore, it is urgently required to replace the fossil fuels with renewable energies such as solar powered electricity.

In recent year, a strong demand for the solar powered electricity leads to increase in solar cell production and shipment. World solar photovoltaic market grew to 5.95 Gigawatts in 2008, representing growth of 110% over the previous year, according to the Solarbuzz (www.solarbuzz.com) report. As a result, the PV industry generated $37.1 billion in global revenues in 2008. So far, the solar cell market is mainly composed of bulk silicon wafer-based solar cells. However, the critical issue in this conventional silicon-based solar cell is still on the expensive electricity rate with 2-3 US $/Wp that should be reduced to less than 1 US $/Wp. Therefore, scientists have been interested in discovering low-cost solar cells. In 1991, a low-cost photovoltaic solar cell with conversion efficiency of 7% was discovered by O'regan and Gratzel, based on TiO_2 nanoparticle and visible light sensitizing material.[2] The cost of this dye-sensitized solar cell (DSSC) was estimated to be 70-80% lower than that of bulk silicon solar cell, indicating that DSSC is the cost-effective technology. Recently, the conversion efficiency has been improved to 10-11%.[3-6] In this paper, nanoengineering technologies of metal oxide particle and film have been reviewed in terms of improving optical property, associated with light harvesting efficiency, and electron transport and life time. Selective positioning of different dyes in a nanostructured TiO_2 film is also introduced.

*E-mail: npark@skku.edu

2. Types of Solar Cells

Solar cell is an electricity generator that converts directly solar light to electricity. Active material comprising solar cell absorbs light, which leads to electron excitation from valence band (or ground state) to con-

duction band (or excited state). Electron-hole charge is separated and then collected at transparent conductive or metallic charge collector. This consecutive process is the basic working principle of solar cell. To separate electron and hole, junction of n-type material (electron acceptor) and p-type material (hole acceptor) is required. From the viewpoint of solar cell materials, there are two types: solid/solid *pn* junction and liquid/solid *pn* junction. Silicon, Copper Indium Selenide (CIS), CdTe, organic bulk heterojunction solar cells belong to solid/solid *pn* junction type. Dye-sensitized solar cell can be categorized as a liquid/solid junction type solar cell that is often referred to as photoelectrochemical cell. Fig. 1 shows the structures and energetics of solid/solid pn junction type and photoelectrochemical type solar cells.

2.1. Dye-Sensitized Solar Cell (DSSC) Structure and Working Principle

Fig. 2 shows the structure and the energy position of each component in DSSC. DSSC consists of the photoanode comprising the dye-adsorbed mesoporous metal oxide (usually TiO_2) film deposited on a transparent conductive oxide (TCO) substrate, the counter electrode composed of a platinum-coated TCO and the iodide/triiodide redox electrolyte. DSSC works as follows. When dye ab-

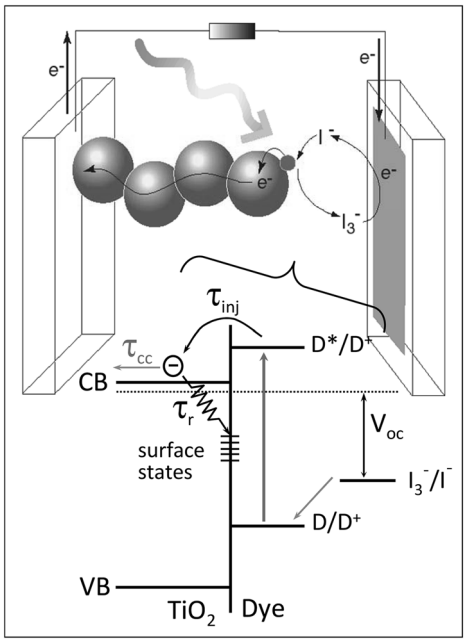

Fig. 2. (Top) DSSC structure consisting of nanoparticulate TiO_2 film, dye, redox electrolyte and Pt counter electrode. (Bottom) Energetics of DSSC and working principle showing electron excitation, electron injection, charge transport and dye regeration.

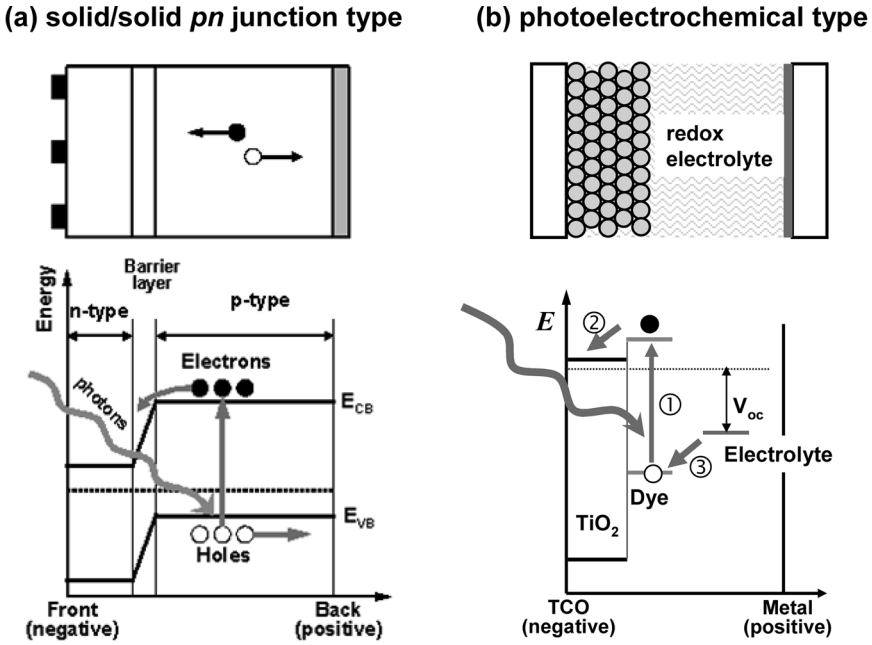

Fig. 1. Structures and energetics of solar cells having (a) solid/solid *pn* junction and (b) liquid/solid *pn* junction showing electron flow.

sorbs photons being equal to or greater than the HOMO-LUMO gap energy, electrons on the HOMO (or ground state) are excited to the LUMO (or excited state) and photo-excited electrons are injected in the conduction band of TiO_2 within pico- to femto-second. The photo-injected electrons are collected at TCO via the porous TiO_2 network by diffusion process with rate of about micro- to mili-second. The oxidized dyes are regenerated by oxidation of iodide within nano-second time scale. Photovoltage is generally determined by the energy difference between the Fermi level of TiO_2 and redox electrolyte potential. Photo-injected electrons can be lost by recombination process through surface states of TiO_2, which has an influence on open-circuit voltage because of tuning of the Fermi energy level.

In DSSC, as mentioned previously, photo-injected electrons are transported by diffusion process since there is no electric filed in the entire TiO_2 film. Under the condition of constant generation of photocharge and removal at the TCO contact, the Fermi energy level decreases in the direction of the back contact (charge collector), especially at short-circuit condition. However, at open-circuit condition the Fermi energy level is constant across the entire film.[7] The photovoltaic action in DSSC is quite different from the conventional solid/solid *pn* junction solar cell,[8] where no significant space charge region id found in DSSC and thereby electric field is not important. Moreover, carrier of only one type is presented in the oxide semiconductor in DSSC compared with coexistence of electron and hole in p-type semiconductor in solid/solid *pn* junction solar cell.

Solar-to-electrical conversion efficiency (η) of DSSC is dependent on short-circuit photocurrent density (J_{SC}), open-circuit voltage (V_{OC}) and fill factor (FF). J_{SC} is resulted form the collective measure of light harvesting efficiency, charge separation efficiency and charge collection efficiency, which depends on materials and nanostructures comprising DSSC.

2.2. Materials for DSSC

Main components for DSSC are nanocrystalline oxide semiconductor, sensitizer, redox electrolyte, counter electrode and transparent conducting oxide. For nanocrystalline metal oxide semiconducting materials, crystallinity, morphology, conduction band energy edge position, nanoparticulate film structure, film porosity and surface area should be taken into carefully consideration. Sensitizer will be better in case that it exhibits panchromatic absorption characteristics with high extinction coefficient. In addition, sensitizer should have a functional group to have chemical bonding on the surface of metal oxide semiconductor. Redox electrolyte is in general composed of I_3^- and I^- ions in non viscous and non volatile solvent. There are numerous materials as I^- source, while iodine (I_2) is the only chemical for I_3^- source. Since TiO_2 conduction band edge is sensitive toward physico-chemical property of electrolyte such as pH, counter cations and additives, formulation of electrolyte is one of important tasks to achieve high efficiency DSSC. Nevertheless, the primary material is metal oxide layer in DSSC because amount of dye adsorption and electrolyte penetration are strongly dependent on nanostructured metal oxide film quality.

3. Metal Oxides for Photoanode in DSSC

3.1. Anatase and rutile TiO_2

When considering metal oxides in order to be applied to photoelectrodes in DSSC, their conduction band energies should be first considered. The conduction band of metal oxide should be lower than the LUMO energy level of sensitizer in order for photo-excited electrons to be injected from dye to metal oxide. For the given Ru-based sensitizer, N719, and iodide/triiodide electrolyte, some of materials can be used as a photoanode material such as ZnO, SnO_2 and Nb_2O_5. Because conduction band edge energies of those materials are lower than the LUMO of N719 and higher than the redox electrolyte potential. Among the several candidates, anatase TiO_2 has demonstrated the best photovoltaic performance with conversion efficiency of more than 10%. For the case of anatase TiO_2, it was reported that the best efficiency could be achieved from exposing nanocrystalline anatase TiO_2 electrodes to a diluted aqueous $TiCl_4$ solution.[9] Post-treated film was usually heated at 500°C. It was therefore assumed that the material formed by $TiCl_4$ post treatment would be anatase TiO_2 phase because anatase was believed to be stable phase at temperature of about 500°C. However, the phase was confirmed to be rutile afterward, where detailed examination was performed on the influence of annealing temperature on the crystal structure, particle size, and particle morphology of TiO_2 films deposited onto SnO_2 conducting glass from the ambient hydrolysis of $TiCl_4$.[10] The rutile TiO_2 particles produced by the ambient hydrolysis of $TiCl_4$ showed rod-like shape which was different from the spherical anatase TiO_2 formed by hydrothermal treatment at around 230°C. It was therefore interested

to draw a comparison between rutile and anatase TiO_2 in terms of morphology-dependent photovoltaic property.

Fig. 3 shows SEM micrographs of the $TiCl_4$-produced rutile TiO_2 film and the anatase TiO_2 film prepared by autoclaving at 230°C using titanium tetra-isopropoxide. The rutile TiO_2 films consists of rod-shaped particles and the typical size of the particles (diameter × length) is about 20 × 80 nm, while anatase TiO_2 shows spherical shape with diameter of about 20 nm. The detailed synthesis was reported elsewhere.[11] As can be seen in Fig. 3, the *J-V* characteristics of dye-sensitized rutile and anatase films (11.5 μm) are compared. Their open-circuit voltages are about the same (730 mV), and J_{SC} of the rutile-based solar cell (10.6 mA/cm^2) is about 30% less than that of the anatase-based cell (14 mA/cm^2). As a result, the energy conversion efficiencies of the rutile- and anatase-based cells are 5.6% and 7.1%. Based on SEM study along with porosity, the surface area of the rutile film is estimated to be at least 25% lower than that of the anatase film. This result suggests that the difference in J_{SC} between rutile- and anatase-based cells is due to difference in surface area, i.e., the amount of dye adsorbed. In addition, the particle packing density is found to have an effect on the electron transport rate. As plotted in Fig. 3, the effective electron diffusion coefficient D_n for the rutile film is about one order of magnitude lower than that of the anatase film, which underlines that electron transport is slower in the rutile layer than in the anatase layer. The difference in the electron transport rate in these materials could be related to two possible factors, i.e., the number of surface states or the extent of interparticle connectivity per unit film volume. The transport of electrons through the nanostructured film is generally accepted to be slowed by multiple trapping events, involving principally surface states.[12-14] The number of surface states is usually in direct proportion to the surface area of a film. If the number of surface states is most important cause in the difference in the rate of electron transport, then it is expected that the surface area of the rutile film would be substantially larger than that of anatase. However, surface area of the rutile film was determined to be smaller than that of the anatase film. Thus, it can be said that the difference in electron transport rate in the rutile and the anatase films is not closely related to the absolute number of surface states. The second possible factor limiting electron transport involves the relative number of interparticle connections. From the cross-sectional morphology of the rutile and the anatase films in Fig. 3, rutile particles are found to be loosely packed, whereas anatase particles are packed closely per unit volume. This implies that the rutile films have a lower number

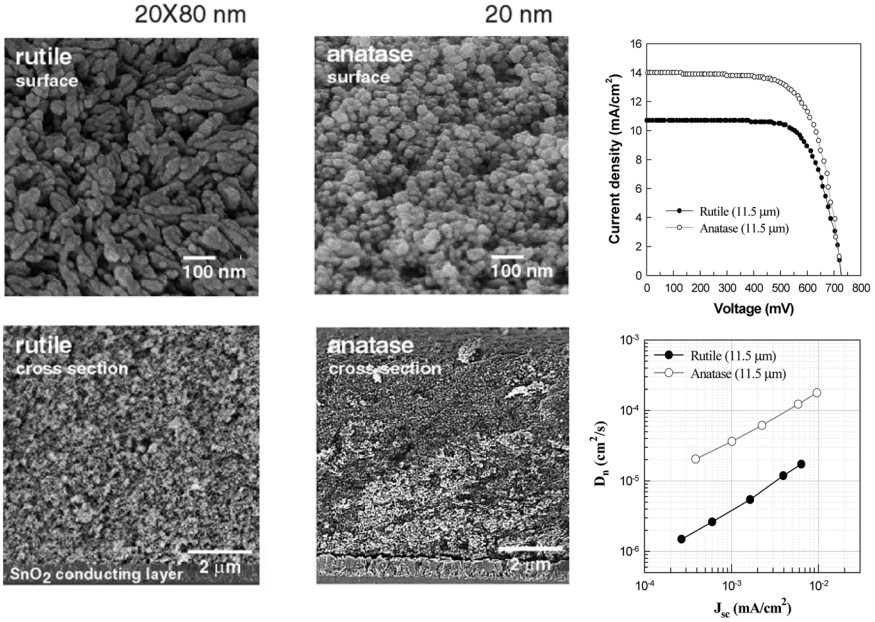

Fig. 3. (Left) Plain-view and cross sectional SEM micrographs of anatase and rutile TiO_2 films. (Right) J-V curves and electron diffusion coefficients of anatase and rutile TiO_2 films.

of interparticle connections per unit film volume than that of the anatase film. Therefore, it is expected that the number of pathways encountered by an individual electron on the way to the charge collector is smaller for a rutile film than for an anatase film. Limiting the number of conductive pathways through the metal oxide particle network is expected to slown electron transport through the rutile film and lower the electron diffusion coefficient. This indicates that film porosity is important to control the electron transport rate in DSSC. The porosity dependence of electron transport behavior was studied in detail.[15)]

3.2. Metal Oxide Particle Size for Light Scattering

As investigated previously, the dye-adsorbed TiO_2 film plays an important role because it serves as a pathway for photo-injected electrons. It is no doubt that the nanocrystalline TiO_2 film with high surface area is able to utilize more photons due to large quantity of the adsorbed dye. However, increase in the surface area by simply increasing the nanocrystalline TiO_2 film thickness is restricted since the increased surface states induced by the increased surface area could act as recombination centers of photo-injected electrons.[16,17)] Instead of using only nanocrystalline TiO_2 particle films, it has been proposed that a double layer structure consisting of light scattering over layer with sub-micron sized particles and nanocrystalline semitransparent TiO_2 under layer. This bi-layer structure can improve photocurrent density because of the improved light scattering effect.[18,19)] Eventually, the scattering effect from the large TiO_2 particles enhances the photocurrent density and thereby overall conversion efficiency. The scattering effect is known to depend on size,[20)] refractive index[19)] and position[21)] of the scattering particles. Therefore, the findings of the correlation between the scattering effect and properties of the scattering particles are important to maximize the scattering efficiency. The scattering efficiency in DSSCs[22,23,24-26)] has been investigated theoretically, in which it is proposed that the scattering is largest when the particle diameter is about $k\lambda$, where k is a constant and λ is the wavelength, that is, light scattering efficiency correlates with the size of the scattering particle. Recently, the size-dependent scattering efficiency in dye-sensitized solar cell has been investigated using a bi-layer film structure.[27)] Two kinds of large scattering particles with rutile phase, G1 and G2 (Showa Denko, Japan), were compared, where particle size of G1 and G2 was about 0.3 μm and 0.5 μm, respectively. The conversion efficiency of 7.55% for the 7 μm-thick TiO_2 film composed of only nanocrystalline TiO_2 was improved to 8.94% and 8.78% after introduction of the scattering layers comprising G1 and G2 particles, respectively. The relatively smaller sized G1 showed higher conversion efficiency than the larger G2 and the improved efficiency was mainly caused by the increase in photocurrent density. Fig. 4(a) shows the IPCE spectra as a function of wavelength. The bi-layer structured film having G1 over layer shows better IPCE than G2 one in the entire wavelength. Fig. 4(b) shows the UV-VIS reflectance of the G1 and G2 particle films. G1 and G2 scattering particles exhibit reflectance as high as 70-80% in the 400-800 nm. The reflectance of the G1 particle film is higher than that of the G2 particle in the 400-700 nm range. On

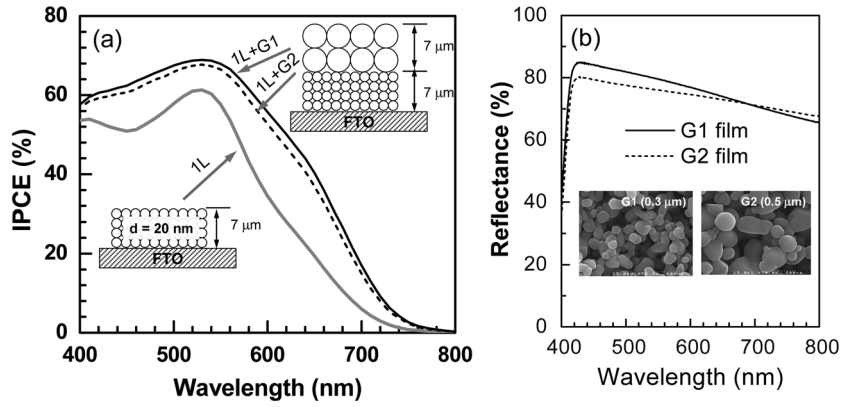

Fig. 4. (a) IPCE spectra of C1- and G2-contained nanocrystalline TiO2 film, along with pure nanocrystalline TiO2 film. (b) Reflectance spectra of G1 and G2 films.

the other hand, G2 has higher reflectance above 700 nm. Therefore, the higher IPCE for the G1 particle over layer than the G2 particle one is ascribed to better reflectance ability of the G1 particle film. Scattering efficiency (h_S) was calculated from the relation $h_S = (T_{ML}) \times (R_{SL}) \times$ (IPCE at under-layer), where T_{ML} and R_{SL} represent transmittance of the under layer and reflectance of the scattering layer, respectively, and each value were taken from the UV-VIS and the reflectance data. The IPCE data without scattering layer were used for the IPCE at the under layer. The calculated scattering efficiency was found to be maximized at around 600 nm, from which scattering efficiency is expected to be maximized when particle size approaches l/2.

3.3. Bi-Functional Metal Oxide

The size of the scattering particle should be large enough to scatter the incident light efficiently since small-size (10-30 nm) nanocrystalline particles cause Rayleigh scattering that is too weak to scatter the light backward.[28] Large TiO_2 particles with spherical shapes or flat surfaces are normally used as the particles for scattering over layer. However, except for their role in scattering of light, electron generation is hardly expected from such a scattering particle with flat surface because of poor dye adsorption property due to the decreased surface area. Therefore, a new functional material is required, which is able to offer both light-scattering and electricity-generation properties. Nano-embossed hollow spherical TiO_2 (NeHS TiO_2) was developed for use in high-efficiency dye-sensitized solar cells.[5] NeHS TiO_2 can be synthesized in basic media. Fig. 5(a) shows SEM images of the as-synthesized NeHS TiO_2 particles. The diameter of the spheres is in the range of 1-3 μm. TEM image shows a hollow-sphere structure with a wall thickness of about 0.25 μm. The surface of NeHS TiO2 is made up of TiO_2 nanoparticles with an average diameter of about 18 nm. To study the bi-functionality of NeHS TiO_2, the NeHS TiO_2 layer was deposited on the nanocrystalline TiO_2 under layer. After introduction of NeHS TiO_2 as an over layer (1L-NeHS), the conversion efficiency was improved by about 21% from 7.79% to 9.43%. When comparing the photovoltaic performance of 1L-NeHS and 1L-CCIC (flat surface scattering particle), 1L-NeHS showed higher J_{SC} and similar V_{OC}, resulting in better conversion efficiency. The higher J_{SC} was probably related to either the amount of adsorbed dye or light scattering or both. The amount of adsorbed dye for the NeHS particles was about 0.58×10^{-7} mol/cm^2, which was about 5 times larger than the amount of 0.12×10^{-7} mol/cm^2 for the CCIC particles. Therefore, the higher J_{SC} observed for 1L-NeHS than 1L-CCIC was attributed to the larger quantity of dye on the NeHS particles. In Fig. 5(b), the UV-VIS reflectance spectrum of the dye-adsorbed NeHS TiO_2 film was compared with those of the dye-adsorbed CCIC TiO_2 one, along with the dye-adsorbed nanocrystalline TiO_2 film. In the short wavelength ranging from 400 to 600 nm, the reflectance of the NeHS TiO_2 film is close to that of the nanocrystalline TiO_2 film, which is mainly

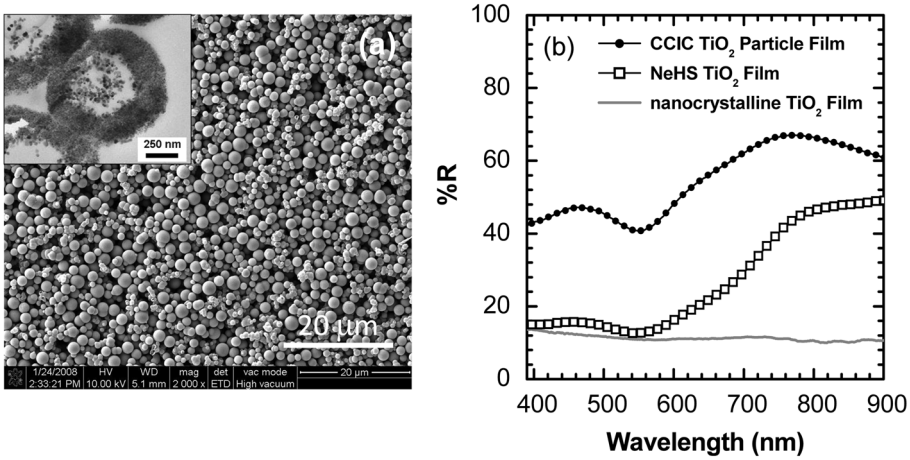

Fig. 5. (a) SEM image of nano-embossed hallow spherical (NeHS) TiO_2. Inset shows TEM image of individual NeHS particle sliced by microtome. (b) Reflectance of the conventional light scattering particle (CCIC) with flat surface and the NeHS particle, along with pure TiO_2 film

due to light absorption by the dye molecules. On the other hand, the CCIC TiO_2 film still shows a high reflectance at 400-600 nm because of low dye adsorption. In the long wavelength region, the dye-adsorbed NeHS film exhibits a substantially higher reflectance than the dye adsorbed nanocrystalline TiO_2 film and its reflectivity is close to that of the CCIC film. Therefore, the improved J_{SC} is caused by both bi-functionality of light scattering and charge generation.

3.4. Nanoengineering for Panchromatic Absorption

Typically, single dye has been used in DSSC. However, sequential adsorption of several dyes in a single TiO_2 mesoporous film is an ideal design to extend the range of light absorption. We developed a new method for selective positioning of organic dye molecules with different absorption ranges in a mesoporous TiO_2 film.[29] The key technology in this method was how to desorb selectively the adsorbed dye, which was started from a simple idea mimicking column chromatography. The polystyrene-filled mesoporous TiO_2 film was explored for use as a stationary phase and a Bronstead base-contained polymer solution was developed for use as a mobile phase for selective desorption of the adsorbed dye. Dye solution and NaOH aqueous solution mixed with polypropylene glycol (PPG) were used as mobile phases for selective adsorption and desorption, respectively. Three dyes used for the experiment were 2-cyano-3-(5-(4-ethoxyphenyl)thiophen-2-yl)acrylic acid (referred to as P5, yellow colour), cis-bis (isothiocyanato) bis (2,2'-bipyridyl-4,4'-dicarboxylic acid) ruthenium(II) (referred to as N719, red colour) and tri(isothiocyanato) (2,2';6',2"-terpyridyl-4,4',4"-tricarboxylic acid) ruthenium (II) (referred to as N749, green colour). Adsorption-desorption procedure was first tested with N719 and N749, which was as follows. N719 dye was first adsorbed on an annealed TiO_2 film, and then polystyrene was formed inside the TiO_2 film to decrease the pore size by means of polymerization of styrene oligomer adsorbed on TiO_2 surface. For selective desorption to remove N719 from the upper region of the TiO_2 film, the desorption solution was prepared by mixing NaOH aqueous solution and poly(propylene glycol) (PPG). The use of PPG was to slow down the penetration rate of NaOH aqueous solution and thereby the thickness of desorbed layer was controlled. N749 dye was adsorbed on the N719-desorbed region. After completion of the selective adsorption, polystyrene was removed by ethyl acetate solution. The developed method realized the selective positioning of three dyes with different absorbance characteristics, P5 (yellow), N719 (red), and N749 (green). Since the longer wavelength light can reach the TiO_2 layer far away from the FTO substrate, the dye alignment was designed to be the following order: FTO/P5/N719/N749. In Fig. 6, EPMA measurements confirm the formation of P5 dye on the bottom of the TiO_2 film, N719 in the middle and N749 on the top. The IPCE spectral shape of the resulting three dyed cell shows well superimposition of each IPCE spectrum from a single dyed cell, as can be seen in Fig. 6. From the J-V measurement, all of the four samples, P5-, N719-, N749- and (P5/N719/N749)-sensitized cells, did not exhibit the same photovoltage. When considering that V_{OC} is determined by the difference between the Fermi energy level of TiO_2 and the redox potential of electrolyte, one might expect that there was little difference in V_{OC} since the same TiO_2 and electrolyte were used for each single dyed cell and three dyed one. Contrary to the expectation, however, all the measured voltages were different. This suggested that the Fermi energy level of TiO_2 was varied with dye when assuming that the redox potential was not changed. We measured electrical impedance spectra. From the second semicircle of the Nyquist plots in electrochemical impedance spectra that has been usually known to be attributed to the back reaction of injected electron transfer at the TiO_2/dye/electrolyte interface,[30,31] it is generally accepted that an increase (or a decrease) in the frequency at the maximum imaginary resistance of the second semicircle (ω_{max}) is related to a decreased (or an increased) V_{OC}, which is due to the accelerated (or retarded) back reaction at open-circuit conditions under illumination. Under the same TiO_2 film thickness and the same electrolyte composition, the V_{OC} will depend logarithmically on reciprocal back reaction constant $1/k_b$.[32] Considering that the ω_{max} is same as the back reaction constant (k_b),[33] the V_{OC} will depend logarithmically on the $1/\omega_{max}$. We found that the observed V_{OC} was proportional to $\ln(1/\omega_{max})$, which suggests that the open-circuit voltage of the solar cell with selectively aligned three different dyes was related to the interfacial charge transfer rate.

4. Summary

Dye-sensitized nanostructured TiO_2 films were investigated. Light scattering method was found to a useful way to utilize long wavelength light, which was dependent on the size of scattering particle, associated with reflectance of scattering particle. Nano-embossed hallow sphere was

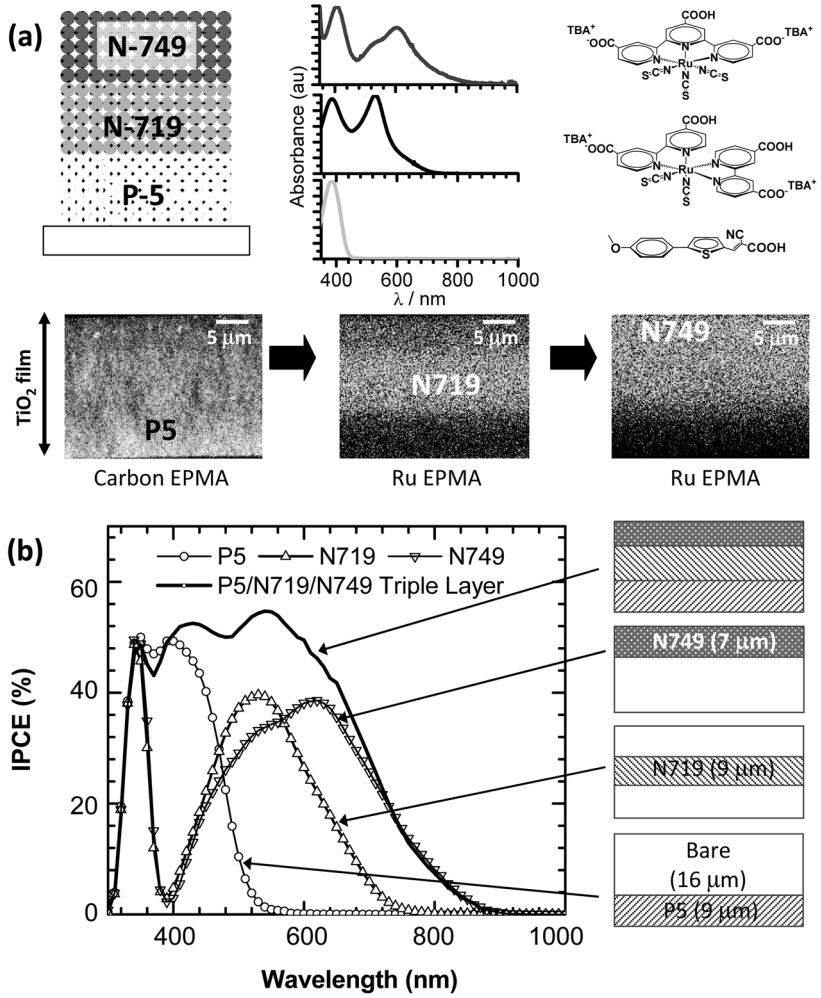

Fig. 6. (a) Selective positioning of three different dyes in a mesoporous TiO_2 film, UV-VIS spectra of P5, N719 and N749 dyes along with their molecular structures and electron probe micro analyzer (EPMA) images during selective positioning of P5, N719 and N749. (b) IPCE spectra of three dyes TiO_2 film along with each dyed TiO_2 film.

one of good candidates for dual functions of both efficient light scattering and charge generation. To cover wide range of incoming light, method of selective positioning of dyes with different absorption characteristics was developed. Selective desorption was realized by controlling retention time of desorption solutions by means of downsizing pore of TiO_2 film and exploring viscous NaOH solution. Panchromatic absorption was realized by this selective positioning of organic sensitizers in a mesoporous inorganic film. This review informed us that nanostructured metal oxide film was primarily important for high efficiency dye-sensitized solar cell.

Acknowledgements

This work was supported by the National Research Foundation of Korea (NRF) grant funded by the Korea government (MEST) (No. 2009-0092950).

References

1. http://en.wikipedia.org/wiki/Richard_Smalley.
2. B. O'Regan and M. Gratzel, 'A low-cost, high-efficiency solar cell based on dye-sensitized colloidal TiO_2 films' *Nature*, **353**, 737 (1991).
3. M. Gratzel, 'Solar energy conversion by dye-sensitized photovoltaic cells' *Inorg. Chem.*, **44**, 6841 (2005).

4. Y. Chiba, A. Islam, Y. Watanabe, R. Komiya, N. Koide, and L. Han, 'Dye-Sensitized solar cells with conversion efficiency of 11.1%' *Jpn. J. Appl. Phys. Part 2*, **45**, L638 (2006).
5. H. -J. Koo, Y. J. Kim, Y. H. Lee, W. I. Lee, K. Kim, and N. -G. Park, 'Nano-embossed hollow spherical TiO_2 as bifunctional material for high-efficiency dye-sensitized solar cells' *Adv. Mater*., **20**, 195, (2008).
6. N. -G. Park and K. Kim, 'Transparent solar cells based on dye-sensitized nanocrystalline semiconductors' *Phys. Stat. Sol. (a)*, **205**, 1895 (2008).
7. J. van de Lagemaat, N. -G. Park, and A. J. Frank, 'Influence of electrical potential distribution, charge transport, and recombination on the photopotential and photocurrent conversion efficiency of dye-sensitized nanocrystalline TiO_2 solar cells: A study by electrical impedance and optical modulation techniques' *J. Phys. Chem. B*, **104**, 2044 (2000).
8. D. Cahen, G. Hodes, M. Gratzel, J. F. Guillemoles, and I. Riess, 'Nature of photovoltaic action in dye-sensitized solar cells' *J. Phys. Chem. B*, **104**, 2053 (2000).
9. C. J. Barbe, F. Arendse, P. Comte, M. Jirousek, F. Lenzmann, V. Shklover, and M. Gratzel, 'Nanocrystalline titanium oxide electrodes for photovoltaic applications' *J. Am. Ceram., Soc*., **80**, 3157 (1997).
10. N. -G. Park, G. Schlichthorl, J. van de Lagemaat, H. M. Cheong, A. Mascarenhas, and A. J. Frank, 'Dye-sensitized TiO_2 solar cells: Structural and photoelectrochemical characterization of nanocrystalline electrodes formed from the hydrolysis of $TiCl_4$' *J. Phys. Chem. B*, **103**, 3308 (1999).
11. N.-G. Park, J. van de Lagemaat and A. J. Frank, 'Comparison of dye-sensitized rutile- and anatase-based TiO2 solar cells' *J. Phys. Chem. B*, **104**, 8989 (2000).
12. P. E. de Jongh and D. Vanmaekelbergh, 'Investigation of the electronic transport properties of nanocrystalline particulate TiO_2 electrodes by intensity-modulated photocurrent spectroscopy' *J. Phys. Chem. B*, **101**, 2716 (1997).
13. N. Kopidakis, E. A. Schiff, N.-G. Park, J. van de Lagemaat, and A. J. Frank, 'Ambipolar diffusion of photocarriers in electrolyte-filled, nanoporous TiO_2' *J. Phys. Chem. B*, **104**, 3930 (2000).
14. J. Nelson, 'Continuous-time random-walk model of electron transport in nanocrystalline TiO_2 electrodes' *Phys. Rev. B*, **59**, 15374 (1999).
15. K. D. Benkstein, N. Kopidakis, J. van de Lagemaat, and A. J. Frank, 'InfluenInflthe percolation network geometry on electron transport in dye-sensitized titanium dioxide solar cells' *J. Phys. Chem. B*, **107**, 7759 (2003).
16. S. Ito, T. Kitamura, Y. Wada, and S. Yanagida, 'Facile fabrication of mesoporous TiO_2 electrodes for dye solar cells: chemical modification and repetitive coating' *Sol. Energy Mater. Sol. Cells*, **76**, 3 (2003).
17. J. Nissfolk, K. Fredin, A. Hagfeldt and G. Boschloo, 'Recombination and transport processes in dye-sensitized solar cells investigated under working conditions' *J. Phys. Chem. B*, **110**, 17715 (2006).
18. S. Ito, S. M. Zakeerudiin, R. Humphry-Baker, P. Liska, P. Charvet, P. Comte, M. K. Nazeeruddin, P. Pechy, M. Takata, H. Miura, S. Uchida, and M. Gratzel, 'High-efficiency organic-dye-sensitized solar cells controlled by nanocrystalline-TiO_2 electrode thickness' *Adv. Mater.*, **18**, 1202 (2006).
19. S. Hore, C. Vetter, R. Kern, H. Smit, and A. Hinsch, 'Influence of scattering layers on efficiency of dye-sensitized solar cells' *Sol. Energy Mater. Sol. Cells*, **90**, 1176 (2006).
20. W. E. Vargas, 'Optimization of the diffuse reflectance of pigmented coatings taking into account multiple scattering' *J. Appl. Phys.*, **88**, 4079 (2000).
21. Z. -S. Wang, H. Kawauchi, T. Kashima, and H. Arakawa, 'Significant influence of TiO_2 photoelectrode morphology on the energy conversion efficiency of N719 dye-sensitized solar cell' *Coord. Chem. Rev.*, **248**, 1381 (2004).
22. A. Usami, 'Theoretical study of application of multiple scattering of light to a dye-sensitized nanocrystalline photoelectrochemical cell' *Chem. Phys. Lett.*, **277**, 105 (1997).
23. A. Usami, 'Theoretical simulations of optical confinement in dye-sensitized nanocrystalline solar cells' *Sol. Energy Mater. Sol. Cells*, **64**, 73 (2000).
24. J. Ferber and J. Luther, 'Computer simulations of light scattering and absorption in dye-sensitized solar cells' *Sol. Energy Mater. Sol. Cells*, **54**, 265 (1998).
25. A. Usami, 'Rigorous solutions of light scattering of neighboring TiO_2 particles in nanocrystalline films' *Solar Energy Mater. Sol. Cells*, **59**, 163 (1999).
26. W. E. Vargas and G. A. Niklasson, 'Optical properties of nano-structured dye-sensitized solar cells' *Sol. Energy Mater. Sol. Cells*, **69**, 147 (2001).
27. H. -J. Koo, J. Park, B. Yoo, K. Yoo, K. Kim, and N.-G. Park, 'Size-dependent scattering efficiency in dye-sensitized solar cell' *Inorg. Chim. Acta*, **361**, 677 (2008).
28. S. Hore, P. Nitz, C. Vetter, C. Prahl, M. Niggemann, and R. Kern, 'Scattering spherical voids in nanocrystalline TiO2-enhancement of efficiency in dye-sensitized solar cells' *Chem. Commun.*, **15**, 2011 (2005).
29. K. Lee, S. W. Park, M. J. Ko, K. Kim, and N. -G. Park, 'Selective positioning of organic dyes in a mesoporous inorganic oxide film' *Nature Mater.*, **8**, 665 (2009).
30. R. Kern, R. Sastrawan, J. Ferber, R. Stangl, and J. Luther, 'Modeling and interpretation of electrical impedance spectra of dye solar cells operated under open-circuit conditions' *Electrochim. Acta*, **47**, 4213 (2002).
31. F. Fabregat-Santiago, J. Bisquert, G. Garcia-Belmonte, G. Boschloo, and A. Hagfeldt, 'Influence of electrolyte in transport and recombination in dye-sensitized solar cells studied by impedance spectroscopy' *Sol. Energy Mater. Sol. Cells*, **87**, 117 (2005).
32. Q. Wang, J. -E. Moser, and M. Gratzel, 'Electrochemical impedance spectroscopic analysis of dye-sensitized solar cells' *J. Phys. Chem. B*, **109**, 14945 (2005).
33. M. Adachi, M. Sakamoto, J. Jiu, Y. Ogata, and S. Isoda, 'Determination of parameters of electron transport in dye-sensitized solar cells using electrochemical impedance spectroscopy' *J. Phys. Chem. B*, **110**, 13872 (2006).